



## ANFIS Controlled Reactive Power Compensation Utilizing Grid-Connected Solar Photovoltaic System as PV-STATCOM

Naveen Gira\* and Anil Kumar Dahiya

Electrical Engineering Department, National Institute of Technology, Kurukshetra 136 119

Received 27 February 2021; revised 07 July 2021; accepted 11 July 2021

This article proposes Adaptive Neuro Fuzzy Inference System (ANFIS) based control scheme for dual use of the grid-connected solar photovoltaic (PV) system as the active power source when irradiance is high and as static compensator (STATCOM) for reactive power compensation to the grid when the irradiance level is inadequate. This way the strategy results in optimal utilization of the converter circuit of the solar PV. Thus, the dual use of solar PV system brings in additional advantages in terms of enhanced power transmission capability of the grid. To examine the efficacy of the proposed control strategy, the system is modeled and analysed in using MATLAB/Simulink tool and also validated over real-time simulator (OPAL-RT-OP5700).

**Keywords:** MATLAB/Simulink, Reactive power compensation, Solar photovoltaic, Static compensator (STATCOM)

### Introduction

Solar PV-based electricity generation has potential at small as well as at large scale. Solar PV generation at the consumer end reduces transmission losses and improves system performance along with environmental benefits. Photo voltaic panels can be installed almost anywhere because of the abundant availability of solar irradiance in most areas of world. In addition, size of solar PV ranges from very small to large ratings depending upon the application.<sup>1</sup> Electricity generated by grid-connected roof-mounted solar PV has significant contribution to the overall electricity generation.<sup>2</sup> When working in grid-tied mode, solar PV power generation requires power-conditioning equipment to convert DC supply into AC. This equipment enables smooth interconnection of solar PV with grid and known as the converter circuit. However, the intermittent availability of solar irradiation results in the underutilization of the interfacing converter connected between AC bus and DC bus. The utilization may improve by supplying reactive power through the same converter circuit. This is achieved by modifying the control technique to deliver the active and reactive power requirements at Point of Common Coupling (PCC).

Modeling of solar PV-STATCOM system compatible with the grid code requirements and

controller capable to operate under normal and faulty conditions has been demonstrated.<sup>3</sup> System stability is also studied in transient operation highlighting the system LVRT capability. A comprehensive review of the issues due to the penetration levels of solar PV into the grid is discussed in Karimi *et al.* (2016)<sup>(4)</sup>, which highlights various issues which solar PV converter face while interfacing with grid.

A PV-STATCOM is implemented in Varma *et al.* (2012)<sup>(5)</sup> with the objective to avoid instability of the induction motor under fault. However, the level of enhancement with the proposed method showcased in the study is reliant on PV size, system strength and loading circumstances. The combination of PV-STATCOM is used in Liu *et al.* 2015<sup>(6)</sup> to mitigate small voltage variations at distribution level. Comparative analysis shows that reactive power control techniques with unbalanced domain are superior to balanced domain. To improve grid power transmission limits with new control techniques of reactive power control are employed in Varma *et al.* (2015).<sup>(7)</sup> The proposed techniques are damping control, voltage control and blend of damping and voltage control. Damping control found to be better than the other two techniques. Night-time application of PV-STATCOM as a reactive power compensation device is explained in Varma *et al.* (2012).<sup>(8)</sup> The proposed techniques results in better utilization of PV generation with reactive power compensation on large-scale generation. In Rezaei & Esmaeili (2017)<sup>(9)</sup>

\*Author for Correspondence  
E-mail: giranaveen@yahoo.com

reactive power control for SPV and wind generation is demonstrated by using Fuzzy based controller. The suggested technique is based on the fuzzy logic, which effectively maintains the per unit voltage by using DGs reactive power ability. However, few functioning issues could not be evaded using given approach and DG's reference voltage needed to vary. Similarly, reactive power control along with reduced harmonics is explained in Seo *et al.* (2009).<sup>(10)</sup> Damping of power oscillations and frequency control using PV-STATCOM is showcased in Varma & Akbari (2020).<sup>(11)</sup> Mitigation of fault induced delayed voltage recovery with the use of PV-STATCOM is demonstrated in Varma & Mohan (2020).<sup>(12)</sup> Implementation of multilevel converter configuration with power quality improvement is demonstrated in Ref<sup>13,14</sup>, all in PV-STATCOM operation mode. The multi-level configuration results in better power quality of inverter supply and smaller filter size requirements, which compensates the cost of additional components required for multiple switches.

Most of the earlier work is concentrated on the large-scale solar PV generation while there is hardly any research available related to the small-scale rooftop grid connected solar PV-STATCOM. The major contribution in this work is to propose a solar PV-STATCOM system that works in grid-connected mode in distribution power system. The converter setup of the solar PV can be utilized as the STATCOM converter to supply real and reactive power during unavailability of solar irradiance. Furthermore, the proposed technique improves the utilization of the converter circuit along with improvement in PCC voltage profile. Although, the complex power supply from the solar PV-STATCOM system is maintained within the converter rating limits, the priority is given to real power. The level of reactive power compensation depends on the available power rating of the converter. Thus, the proposed system can supply maximum reactive power in the night-time and limited reactive power in the daytime. A single source infinite-bus system is simulated to study the capability of the suggested control method. This work proposes the control scheme of an ANFIS based controller<sup>15-19</sup> in Synchronous Reference Frame (SRF) theory. The ANFIS based control of solar PV-STATCOM has advantages such as adaptability and robustness. The ANFIS based maximum power point tracking is capable of providing optimum power from solar PV at variable irradiance.<sup>20</sup> Simulations are executed in the

MATLAB/Simulink and OPAL-RT real-time simulator (RTS) to highlight the ability of the suggested control technique for variable irradiance levels and loads. The night-time operation is also simulated by reducing the irradiance to zero level.

### System Modeling

The single-line illustration of the proposed grid-connected solar PV-STATCOM system is displayed in Fig. 1. A DC-DC converter is connected to increase the DC voltage level between the solar PV panel and DC link capacitor. The LCL filter, which also serves as the STATCOM inductor, is coupled between the PCC and the converter circuit. The combination of variable active and reactive load is connected to PCC through the circuit breaker.

### Solar PV System

A solar PV cell is modeled as p-n junction diode connected in shunt with current source and shunt resistance and in series with series resistance named as  $R_s$ ,  $R_{sh}$ , is shown in Fig. 2. Solar cells are connected to form solar PV module parallel or series PV cells. Solar PV modules are combined in series and parallel as solar PV array in order to increase current and voltage outputs. Equations (1-2) represents the reverse saturation current ( $I_{rr}$ ) and PV output current ( $I_o$ ), respectively. Diode saturation current ( $I_d$ ) is in direct relation with the solar panel surface temperature as in Eq. (3).

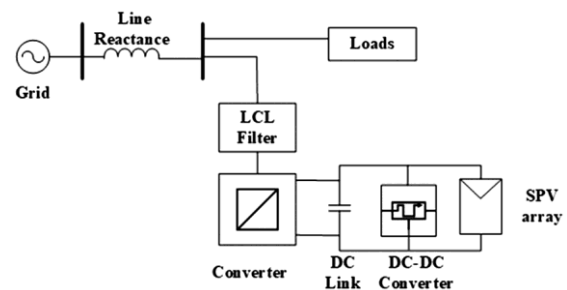


Fig. 1 — A single line representation of solar PV-STATCOM in power system

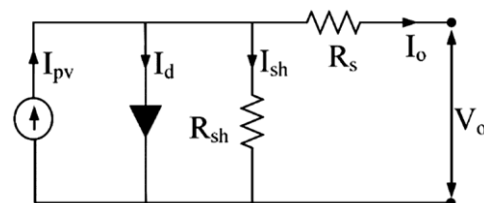


Fig. 2 —Single diode solar cell model

$$I_o = I_{pv} - I_d \left[ \exp \left\{ \frac{q(V_o + I_o R_s)}{N_s A K T_{ak}} \right\} - 1 \right] \quad \dots (1)$$

$$I_{rr} = \left[ \frac{I_{scr}}{\exp \left( \frac{qV_{oc}}{KAN_s T_{rk}} \right) - 1} \right] \quad \dots (2)$$

$$I_d = I_{rr} \left( \frac{T_{ak}}{T_{rk}} \right)^3 \exp \left( \frac{qE_g}{KA} \right) \left( \frac{1}{T_{rk}} - \frac{1}{T_{ak}} \right) \quad \dots (3)$$

where,  $I_{rr}$ ,  $I_{scr}$ ,  $I_o$ ,  $I_{sc}$ ,  $I_{pv}$ ,  $I_d$ ,  $I_{sh}$  are reverse saturation current, module short circuit current, PV current, short circuit current, PV output current, diode saturation current and shunt current respectively.  $V_{oc}$  and  $V_o$  are open circuit voltage and PV output voltage correspondingly. Reference temperature ( $^{\circ}K$ ) and actual temperature ( $^{\circ}K$ ) respectively are denoted by  $T_{rk}$ ,  $T_{ak}$ . Parallel resistance and series resistance respectively are denoted by  $R_{sh}$ ,  $R_s$ . Number of cells in series is denoted by  $N_s$  whereas  $E_g$  denotes band gap energy of material used (1.12 eV (Si)),  $A$  is the diode ideality constant,  $q$  is charge of electron ( $1.6021 \times 10^{-19}$  C),  $K$  is Boltzmann constant ( $1.38065 \times 10^{-23}$  JK $^{-1}$ ).

Every curve of voltage-current characteristics contains a unique point where maximum power is attained. This point is identified as Maximum Power Point (MPP). At MPP the corresponding voltage and current are known as MPP voltage ( $V_{mpp}$ ) and MPP current ( $I_{mpp}$ ), respectively. A DC/DC boost converter boosts a low voltage into voltage of higher magnitude. A straightforward link between the boost converter output voltage and duty ratio is established in Eq. (4).

$$V_{out} = \frac{V_{in}}{1 - D} \quad \dots (4)$$

where  $V_o$ ,  $V_{in}$  are the output voltage and input voltage of the converter respectively. Output Current is  $I_o$ . The objective of the converter is to operate the solar PV at MPP under variable irradiance. The duty cycle of the DC-DC converter is calculated according to the voltage and current of the solar PV array. The variation in duty cycle results in the pulse width modulation (PWM) switching of the device. An ANFIS based MPPT method is applied to obtain the maximum power point.<sup>21</sup> The DC link voltage is however sustained by the solar PV-STATCOM controller.

### LCL Filter Design

LCL filter is connected between the DC/AC converter and the low voltage distribution power system. The calculation of filter components is given in this section.<sup>22</sup> Capacitor value can be calculated as Eq. (5),

$$C_f = k \frac{1}{\omega_g Z_b} \quad \dots (5)$$

where,  $C_f$  is filter capacitance,  $k$  is rating factor and its value is considered to be less than 5 percent of base capacitance.<sup>22</sup> Here  $\omega_g$  is the fundamental angular frequency of the system and  $Z_b$  is system base impedance. The filter inductor value is calculated in Eq. (6),

$$L_f = \frac{V_{dc}}{6 f_{sw} \Delta I_{Lmax}} \quad \dots (6)$$

where,  $V_{dc}$  is known as DC link voltage,  $\Delta I_{Lmax}$  is given as peak-to-peak current ripple and  $f_{sw}$  as switching frequency of PWM based current regulator.

### STATCOM

STATCOM mainly compensates the reactive power at PCC to regulate the voltage and to improve stability of power systems. Simultaneously, DC power of the solar PV panel is converted into AC power utilizing the STATCOM converter. The basic components of the STATCOM are: an inductor, a DC link capacitor, and a converter circuit. Reactive power compensation is accomplished by varying the current through the inductor connected between the grid and STATCOM converter. The current is controlled by pulses generated using the PWM generator.

### Controller Modeling

The main purpose of the STATCOM in the AC grid is to maintain the power flow from the DC-link capacitor to AC grid at PCC and vice versa. A well-known d-q reference controller helps in achievement of the desired performance of STATCOM<sup>10</sup>, as depicted in Fig. 3. The DC voltage, PCC current, and PCC voltage are the input parameters fed to the controller. With the help of Phase-Locked Loop (PLL), angle ( $\theta$ ) is calculated to estimate the d-q parameters. The result from subtraction of predefined voltage and instantaneous voltage value is used to compute the reference current  $I_Q^*$ . To retain DC link voltage, it is observed and compared with the reference voltage  $V_{dc}$ , then the reference current  $I_D^*$  is generated. The multiplication of  $\cos \theta$  and  $\sin \theta$  with

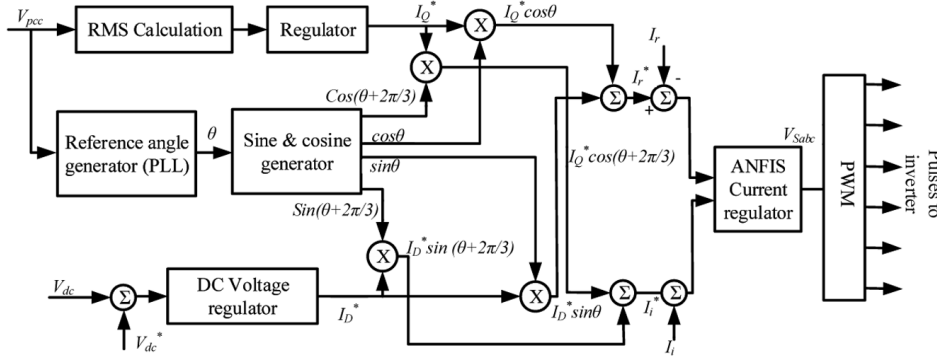


Fig. 3 —Block diagram of STATCOM controller

| Component | Parameter                    | Value                                   |
|-----------|------------------------------|---|
| Grid      | Voltage                      | 120 kV, 50Hz                            |
|           | Short circuit current rating | 50 MVA                                  |
| Line      | Resistance                   | 0.0127 Ω/kM                             |
|           | Inductance                   | 0.933 H/kM                              |
| STATCOM   | LCL Filter <sup>23,24</sup>  | 0.007142×2 H,<br>0.7×10 <sup>-6</sup> F |
|           | Voltage Rating (AC/DC)       | 400 V RMS / 700V                        |
|           | Capacitor                    | 0.9 mF                                  |
| Load      | Maximum Power                | 4.5 kW, 0.9 kVAR                        |
| PV Array  | P <sub>Max,0</sub>           | 640 W                                   |
|           | V <sub>OC,0</sub>            | 21.1 V                                  |
|           | I <sub>SC,0</sub>            | 3.8 A                                   |
|           | No. of cells in Module       | 2×287                                   |

$I_Q^*$  and  $I_D^*$ , respectively is used to calculate essential real current  $I_r^*$ . The requisite imaginary current  $I_i^*$  can also be achieved by multiplication of  $\cos(\theta+2\pi/3)$  and  $\sin(\theta+2\pi/3)$  with  $I_Q^*$  and  $I_D^*$  respectively. The imaginary and real components of DSTATCOM current are subtracted from requisite  $I_Q^*$  and  $I_D^*$  to regulate the current deviations. Then, the generated voltages ( $V_{Sabc}$ ) output from controller are fed to PWM generator to generate the triggering pulses of the converter switches. The q-axis component is utilized for reactive power compensation and voltage regulation. The d-axis component is used to maintain the consistent level of DC voltage using active power control. Both the reactive and active powers are controlled simultaneously. The ratings of various system components are given in Table 1.

In this research, the proposed ANFIS based control is outlined utilizing MATLAB/Simulink, the Artificial Neural Network (ANN) is trained using back propagation (BP) learning technique. BP learning technique is a repetitive method utilizing gradient descent process all together to limit the square error among the desired and actual results for a specified training data set, which results in updated

parameters of given system for a repetitive manner starting from last layer and reaching to initial hidden layer. The ANFIS have characteristics of general fuzzy framework with the exception that estimation at each stage is achieved in hidden layer by the neurons and subsequently the ANN training is utilized to support the information of the framework. The ANFIS control configuration utilizes Sugeno-type framework with the constraints encompassed by BP based neural system. The ANFIS associates the benefits of fuzzy and adaptive networks in the hybrid intelligent paradigm.

**Results and Discussion**

The effectiveness of the control strategy is verified using MATLAB/Simulink as well as RTS and discussed in the following subsections.

**MATLAB based Simulation Results**

The detailed simulations for different operating conditions are executed in the MATLAB/Simulink as highlighted in Fig. 4(a-i). The STATCOM is operating with the grid throughout the simulation period, whereas the SPV is coupled to the DC link at  $t = 500$  ms. The solar irradiance is reduced to  $0 \text{ w/m}^2$  at  $t = 2800$  ms to imitate night-time operation, as displayed in Fig. 4(a). At  $t = 750$  ms, the load is varied from  $3.5 + j0.500 \text{ kVA}$  to  $4.5 + j0.900 \text{ kVA}$  for  $t = 1450$  ms, as illustrated in Fig. 4(b). The load is again varied from  $3.5 + j0.500$  to  $4.5 + j0.900 \text{ kVA}$  at  $t = 2800$  ms, during zero irradiance period. The active and reactive power yield of the solar PV-STATCOM is depicted in Fig. 4(c). The modified solar system supplies active power and compensates the reactive power demand of the variable load simultaneously. Therefore, the active power demand on the grid is reduced when using the solar PV-STATCOM, as displayed in Fig. 4(d). The modified solar system itself meets the reactive power requirement of the

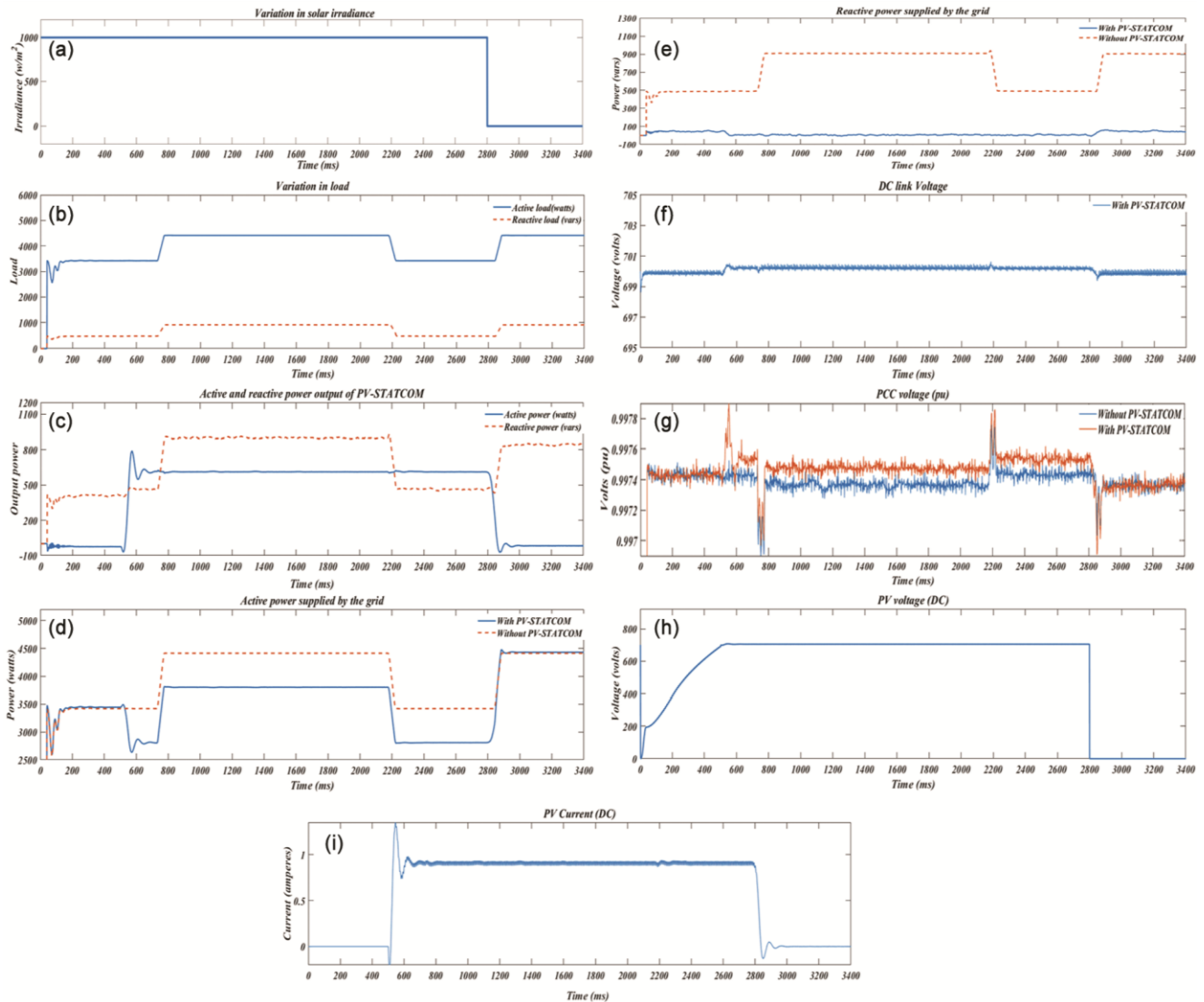


Fig. 4 — (a) Variation in solar irradiance, (b) Variation in active and reactive load, (c) Reactive and active power provided from PV-STATCOM to Load, (d) Active power supplied by the grid to load, (e) Reactive power delivered from grid to the load, (f) DC link voltage, (g) The per unit voltage at PCC, (h) Solar PV array output current, (i) Solar PV array output voltage

load and therefore, the reactive power drawn from the grid becomes almost negligible, as depicted in Fig. 4(e). The reactive power compensation is most effective near the consumer connection because it reduces the VA burden on the grid, which results in superior operation of distribution power system. The DC link voltage remains immune to the variation in irradiance and load as displayed in Fig. 4(f). The per unit voltage variation at the PCC with and without the SPV-STATCOM is demonstrated in Fig. 4(g). As displayed in Fig. 4(g), the voltage profile improves due to reactive power compensation at PCC. The voltage regulation of the power system also improves due to the reactive power compensation

at the PCC. The magnitude of the DC voltage of boost converter remains constant during load variations as shown in Fig. 4(h). The wave form of solar PV output current displayed in Fig. 4(i), explains that the PV current reduces to zero when irradiance becomes zero at  $t = 2800$  ms. ANFIS controller enables the solar PV-STATCOM to compensate reactive power according to load requirement and to provide constant real power throughout the daytime as displayed in Figs. 4(c-e). Additionally, a constant DC link voltage (700V) is maintained throughout the simulation, barring small fluctuations. The solar PV supplies a DC current of 0.9 A at the rated irradiance level and the current

reduces to zero at zero irradiance level. During this period ( $t = 2800\text{--}3400\text{ ms}$ ) the solar PV-STATCOM supplies only reactive power (Fig. 4(c)), depicting the efficacy of the proposed setup.

**Validation of Simulation Results in RTS**

Validation of simulation results is carried out in this section with the help of the real-time simulator of OPAL-RT. The real-time simulator are gathering prominence for validation of complex power system performance.<sup>25,26</sup> The proposed system is authenticated in RT-LAB interface of OPAL-RT interrelated with MATLAB/Simulink as displayed in Fig. 5(a). The lab based OPAL-RT setup is demonstrated in Fig. 5(b). It consists of a PC-based real time system target and a host computer. The host computer includes an Intel core (TM) i7 processor, 4 GB RAM and a 64-bit operating system. The simulations are executed using MATLAB/Simulink 2013b, uploaded on RT-LAB interface of Opal-RT-OP5700. Real time results are comparable to hardware prototype outcomes.

The ether-net cable transmits data amid the real-time digital simulator setup and host computer. The

load is varied from  $3.5 + j0.500$  to  $4.5 + j0.900\text{ kVA}$ , as illustrated in Fig. 6(a). The load is again varied from  $3.5 + j0.500$  to  $4.5 + j0.900\text{ kVA}$  during zero irradiance. The active and reactive power output waveform of the SPV-STATCOM is depicted in Fig. 6(b). The active and reactive power demand to grid is reduced if SPV-STATCOM is used, as displayed in Fig. 6(c) and 6(d). DC link voltage remains constant throughout the simulation as represented in Fig. 6(e). The results from real time simulations display that the setup and controllers are ready to be utilized in the hardware based environment.

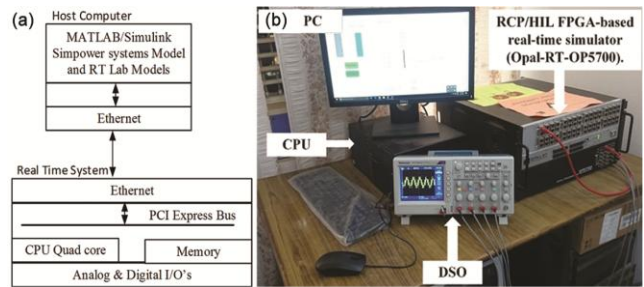


Fig. 6 —(a) Setup Architecture, (b) Test setup

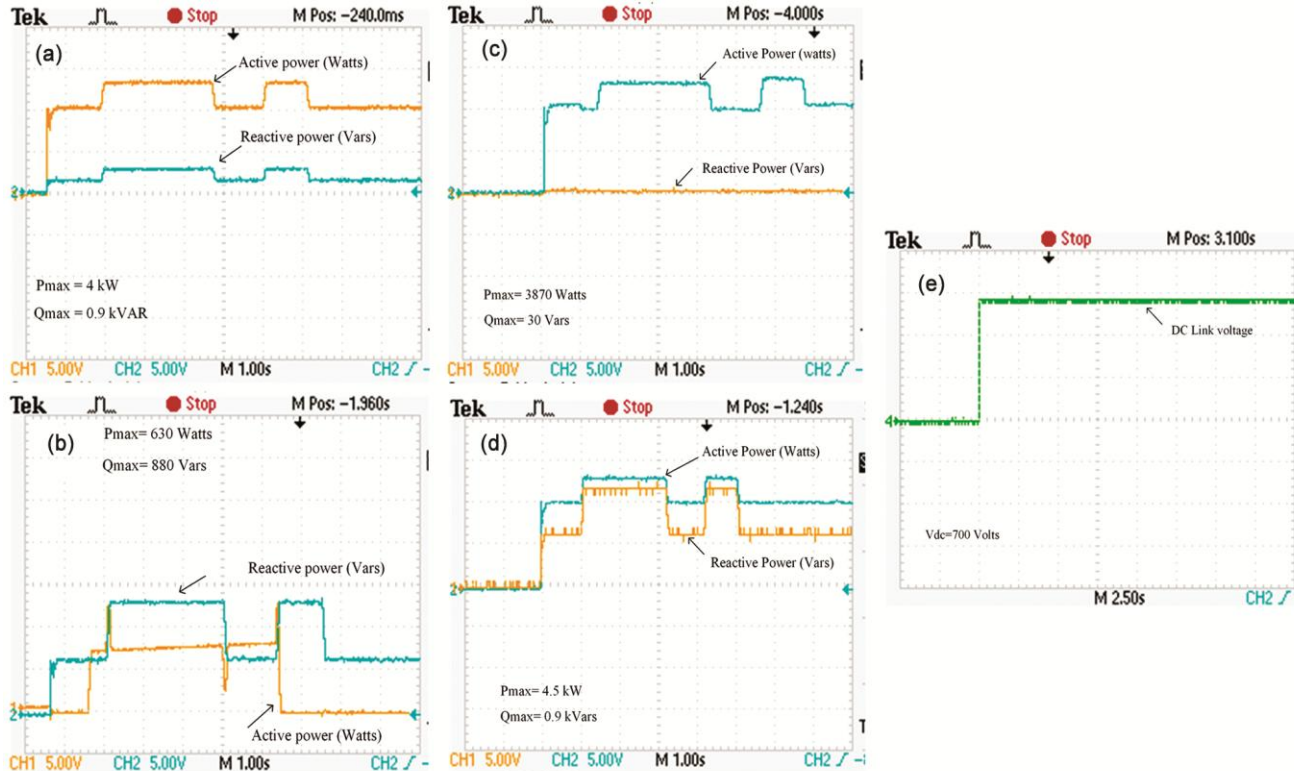


Fig. 5 — (a) Variation in active and reactive load, (b) Active and reactive power supplied by PV-STATCOM to load, (c) Active and reactive power delivered by grid when PV-STATCOM is connected, (d) Active and reactive power delivered by grid when PV-STATCOM is disconnected, (e) DC link voltage



## Conclusions

In this study, the solar PV converter is utilized as a STATCOM converter to supply active and reactive power at the PCC. A detailed model of the solar PV-based STATCOM is simulated on MATLAB/Simulink platform. The system operation is validated in the RT-LAB using OPAL-RT. The simulation study is performed for variable irradiance levels and loads. The solar PV-STATCOM controller is based on ANFIS, which is robust and adaptive. The simulation results indicate that the solar PV-based STATCOM supplies active power at the PCC during the daytime, additionally, the solar PV-STATCOM is effective for compensating reactive power under variable load conditions during the day and night. The simulation results also indicate that voltage at the PCC is improved although marginally by using the solar PV-STATCOM. For the future work, the performance of the proposed system can be further improved by using storage devices connected at the DC bus and selective parameter control for economic operation of the proposed setup.

## References

- 1 Tabasi M & Bakhshinejad A, A novel high voltage gain and low voltage stress DC-DC boost converter for photovoltaic applications, *Majlesi J Electr Eng*, **12** (2018) 47–54.
- 2 RETA, 2016, *Grid Parity of Solar PV Rooftop Systems for the Commercial and Industrial Sectors: New Delhi* (The Energy and Resources Institute) 2016, 172.
- 3 Nanou S I & Papathanassiou S A, Modeling of a PV system with grid code compatibility, *Electr Power Syst Res*, **116** (2014) 301–310.
- 4 Karimi M, Mokhlis H, Naidu K, Uddin S & Bakar A H A, Photovoltaic penetration issues and impacts in distribution network – A review, *Renew Sustain Energy Rev*, **53** (2016) 594–605.
- 5 Varma R K, Rahman S A, Sharma V & Vanderheide T, Novel control of a PV solar system as STATCOM (PV-STATCOM) for preventing instability of induction motor load, *25th IEEE Can Conf Electr Comput Eng*, 2012, 1–5.
- 6 Liu X, Cramer A M & Liao Y, Reactive power control methods for photovoltaic inverters to mitigate short-term voltage magnitude fluctuations, *Electr Power Syst Res*, **127** (2015) 213–220.
- 7 Varma R K, Rahman S A & Vanderheide T, New control of PV solar farm as STATCOM (PV-STATCOM) for increasing grid power transmission limits during night and day, *IEEE Trans Power Deliv*, **30** (2015) 755–763.
- 8 Varma R K, Rahman S A, Mahendra A C, Seethapathy R & Vanderheide T, Novel nighttime application of PV solar farms as STATCOM (PV-STATCOM), *IEEE Power Energy Soc Gen Meet* 2012, 1–8.
- 9 Rezaei F, Esmaili S, Decentralized reactive power control of distributed PV and wind power generation units using an optimized fuzzy-based method, *Int J Electr Power Energy Syst*, **87** (2017) 27–42.
- 10 Seo H, Kim G-H, Jang S, Kim S, Park S, Park M & Yu I-K, Harmonics and reactive power compensation method by grid-connected Photovoltaic generation system, *Int Conf Electr Mach Syst* 2009, 1–5.
- 11 Varma R K, Akbari M, Simultaneous fast frequency control and power oscillation damping by utilizing PV solar system as PV-STATCOM, *IEEE Trans Sustain Energy*, **11** (2020) 415–425.
- 12 Varma R K & Mohan S, Mitigation of fault induced delayed voltage recovery ( FIDVR ) by PV-STATCOM, *IEEE Trans Power Syst*, **35** (2020) 4251–4262.
- 13 Sridhar V & Umashankar S, A comprehensive review on CHB MLI based PV inverter and feasibility study of CHB MLI based PV-STATCOM, *Renew Sustain Energy Rev*, **78** (2017) 138–156.
- 14 Hussain I, Kandpal M & Singh B, Grid integration of single stage SPV-STATCOM using cascaded 7-level VSC, *Int J Electr Power Energy Syst*, **93** (2017) 238–252.
- 15 Awadallah M A, Soliman H M, A neuro-fuzzy adaptive power system stabilizer using genetic algorithms, *Electr Power Components Syst*, **37** (2009) 158–173.
- 16 Semero Y K, Zheng D & Zhang J, A PSO-ANFIS based hybrid approach for short term PV power prediction in microgrids, *Electr Power Components Syst*, **46** (2018) 95–103.
- 17 Sharma G, Nasiruddin I, Niazi K R & Bansal R C, ANFIS based control design for AGC of a hydro-hydro power system with UPFC and hydrogen electrolyzer units, *Electr Power Components Syst*, **46** (2018) 406–417.
- 18 Badoni M, Singh A & Singh B, Design and implementation of adaptive neuro-fuzzy inference system based control algorithm for distribution static compensator, *Electr Power Components Syst*, **43** (2016) 1741–1751.
- 19 Awadallah M A & Morcos M M, Diagnosis of open-phase faults in PM brushless DC motors using wavelet and adaptive fuzzy techniques, *Electr Power Components Syst*, **32** (2004) 1165–1190.
- 20 Naveen & Dahiya A K, Implementation and comparison of Perturb & observe, ANN and ANFIS based MPPT techniques, *Int Conf Inven Res Comput Appl* 2018, 1–5.
- 21 Nayak M & Reddy V, A quick and effective MPPT scheme for solar power generation during dynamic weather and partial shaded conditions, *Eng Sci Technol an Int J*, **22** (2019) 869–884.
- 22 Reznik A, Simoes M G, Al-Durra A, Muyeen S M, LCL filter design and performance analysis for grid-interconnected systems, *IEEE Trans Ind Appl*, **50** (2014) 1225–1232.
- 23 Saïd-Romdhane M Ben, Naouar M W, Belkhdja I S & Monmasson E, Simple and systematic LCL filter design for three-phase grid-connected power converters, *Math Comput Simul*, **130** (2016) 181–193.
- 24 Tavakoli Bina M & Pashajavid E, An efficient procedure to design passive LCL-filters for active power filters, *Electr Power Syst Res*, **79** (2009) 606–614.
- 25 Ahmad Z & Singh S N, Improved modulation strategy for single phase grid connected transformerless PV inverter topologies with reactive power generation capability, *Sol Energy*, **163** (2018) 356–375.
- 26 Subudhi B & Ogeti P S, Optimal preview stator voltage-oriented control of DFIG WECS, *IET Gener Transm Distrib*, **12** (2018) 1004–1013.